Superconducting and normal states of $Ba_{1-x}K_xBiO_3$ studied with use of high-quality thin films

H. Sato,* T. Ido, and S. Uchida
Department of Applied Physics, University of Tokyo, Yayoi 2-11-16, Bunkyo-ku, Tokyo 113, Japan

S. Tajima and M. Yoshida
Superconductivity Research Laboratory, International Superconductivity Technology Center, Shinonome 1-10-13, Koto-ku, Tokyo 135, Japan

K. Tanabe
Nippon Telegraph and Telephone Interdisciplinary Research Laboratories, Tokai, Ibaraki 319-11, Japan

K. Tatsuhara and N. Miura
Institute of Solid State Physics, University of Tokyo, Roppongi, Minato-ku, Tokyo 106, Japan
(Received 13 July 1992; revised manuscript received 14 May 1993)

An extensive study of $Ba_{0.55}K_{0.45}BiO_3$ thin films is reported, including precise measurements of the transport coefficients, the reflectivity spectrum, the Raman spectra, the upper critical field, and the superconducting energy gap. From the results for the normal-state properties, it is suggested that the electronic state in the metallic phase of $Ba_{1-x}K_xBiO_3$ can be described by a simple band picture. The measurement of the superconducting-state properties shows good consistency with this picture within the BCS framework. Based on these experimental results, we firmly conclude that the density of states in the conduction band of $Ba_{1-x}K_xBiO_3$ is close to that expected from a band model in its metallic phase and the superconductivity is of BCS type. The coupling strength $\lambda \sim 1$ is also estimated from the gap measurements and the temperature dependence of the resistivity.

I. INTRODUCTION

The superconductivity in the Ba-K-Bi-O system above 20 K was discovered by Mattheiss, Gyorgy, and Johnson.[1] The superconducting phase was identified by Cava *et al.*[2] as the perovskite oxide $Ba_{1-x}K_xBiO_3$, in which the superconducting transition temperature has exceeded 30 K. This is the highest transition temperature reported so far except those in the cuprate superconductors and the alkali-metal-doped C_{60}.[3]

The high-temperature superconductivity in this system has attracted much interest because it contains neither Cu atoms nor a two-dimensional structural feature, which are considered to be crucial conditions for the high transition temperature in oxide materials. To distinguish similarities and differences in the high-T_c Cu oxides and clarify the mechanism of the high-temperature superconductivity in $Ba_{1-x}K_xBiO_3$, it is essential to investigate physical properties of this system in both the superconducting and normal state.

Because of difficulty in preparation of sintered samples with enough quality in this system, earlier studies were confined to experiments on powder samples or sintered samples with low density such as structural analysis by diffraction methods,[2,4] measurements of the magnetic properties,[5,6] and isotope effect measurements.[5,7,8] These studies established the basic understanding for the $Ba_{1-x}K_xBiO_3$ system as follows. (1) Only the superconducting phase has a simple cubic structure. (2) The electronic specific-heat coefficient for the superconducting phase is 1–2 mJ/mole f.u. and much smaller than those in the high-T_c Cu oxides. (3) A BCS-like isotope effect is observed for the superconductivity. (4) There is no local moment.

In the next stage, Hinks *et al.* succeeded in synthesizing high-quality sintered samples through a melt-cast process in a reducing atmosphere.[9] Using the high-density sintered samples, measurements of optical, Raman, and tunneling spectra were performed.[10–13]

The optical measurement[10] and the point-contact tunneling measurement[13] showed a BCS-like superconducting energy gap with $2\Delta/k_BT_c = 3.5$–4.5. However, the resistivity of the sintered samples were larger than 10 mΩ cm indicating a serious effect of grain boundaries, which is fatal for transport measurements[14] or fabrication of sandwich-type tunnel junctions.[12] Recently the growth techniques of thin films[15–18] and single crystals[19] has been developed and applied to tunneling studies with sandwich-type junctions.[18,20,21]

We have attempted to overcome the difficulty in sample preparation by synthesis of highly oriented thin films by sputtering and performed the measurements of their physical properties. In our preceding reports,[15,20,22] the results of optical and transport measurements in the normal state indicated that the splitting of the conduction band observed in $BaBiO_3$ disappears in the metallic phase of $Ba_{1-x}K_xBiO_3$. This situation is significantly different from the case of the B-site substituted Bi oxide, $BaBi_{1-x}Pb_xO_3$, and the copper-oxide superconductors, in which the energy gap generated by either charge-density wave (CDW) or the strong electron correlation is preserved to some extent even in the metallic phase. For

the superconducting state, the conductance spectrum for a tunnel junction fabricated on a $Ba_{0.55}K_{0.45}BiO_3$ thin film showed that this material is a BCS-type superconductor with a finite-energy gap.[20] But a complete discussion which covers both of normal and superconducting states has not yet been done.

In this work, we report more extensive investigation on superconducting $Ba_{0.55}K_{0.45}BiO_3$ films with improved quality including measurements of the transport coefficients, the reflectivity spectrum, the Raman spectra, the upper critical field, and the superconducting energy gap. The consistency among the parameters for the superconducting and the normal states obtained from these experimental results give quantitative evidence that the density of states of the conduction band in $Ba_{0.55}K_{0.45}BiO_3$ is close to that expected from the band calculations,[23] and the superconductivity in this system is of the BCS type. The strength of the electron-phonon coupling is also estimated as $\lambda \sim 1$.

II. GROWTH OF THE THIN FILMS

The $Ba_{0.55}K_{0.45}BiO_3$ thin films were grown by rf-magnetron sputtering from sintered targets ($3''\phi$) with a cation ratio Ba:K:Bi=0.3:0.7:0.7. A mixture of argon and 1% oxygen was used as the sputtering gas with total pressure 5–20 mTorr. The (110) and (100) $SrTiO_3$ substrates were set on a stainless-steel heater block facing the surface of the target. The distance between the target and the substrates was 6.5 cm. In the most of the run, the substrates were attached with silver paste or indium metal to the heater block which was held at a temperature between 300 and 500 °C during the growth. The rf sputter source was operated with rf power of 80 W, resulting in a deposition rate of 1.7 Å/s. The deposition was made for 0.5 h, producing a total film thickness of 3000 Å. Because of the reducing growth conditions, the films had large numbers of oxygen vacancies; these were filled by annealing the films in flowing oxygen at temperatures between 450 and 500 °C for 1 h.

The chemical composition of the films were determined roughly by electron-probe microanalysis and x-ray fluorescence analysis. In particular, the K coposition x was estimated from the lattice constant.[24] The x-ray-diffraction patterns indicated that the films included no secondary phase and that the thin films on (110) and (100) $SrTiO_3$ substrates were perfectly oriented in the (110) and (100) directions, respectively. The films exhibited superconducting transition between 20 and 23 K with the transition width narrower than 0.5 K.

III. ELECTRICAL RESISTIVITY

We measured the resistivity of the $Ba_{0.55}K_{0.45}BiO_3$ thin films by the four-probe method. The electrodes were formed by evaporating gold on the as-sputtered films before the oxygen annealing. After the annealing procedure, the contact resistance of the gold electrodes was lower than 1 Ω, which was sufficient for the transport measurements.

The resistivity of the $Ba_{0.55}K_{0.45}BiO_3$ thin films was sensitive to the temperatures during film growth and annealing procedure as shown in Figs. 1(a) and 1(b). The growth conditions of the films in Fig. 1 were summarized in Table I. The films grown at the lower substrate and annealing temperatures has the lower resistivity and positive temperature coefficient of resistivity. In sample j, the resistivity is 240 μΩ cm at room temperature and 140 μΩ cm at 30 K. These values are the lowest among those reported so far for $Ba_{1-x}K_xBiO_3$ except for the thin films grown by a laser deposition technique.[18] The temperature coefficient of resistivity is always positive in sign from 300 K to T_c and the absolute value was 0.26 μΩ cm/K at 300 K. As shown in Fig. 1(a), the metallic temperature dependence of resistivity is observed over the whole temperature range for samples j, i, and h when the resistivity at 300 K is lower than 700 μΩ cm. It should be noted that the slopes of the resistivity in all the metallic samples were almost parallel so that the differences of resistivity among the films were temperature independent. On the other hand, in the films for which the resistivity was much higher than 700 μΩ cm, samples $a-e$, the resistivity increased with temperature.

No systematical difference can be seen among the x-

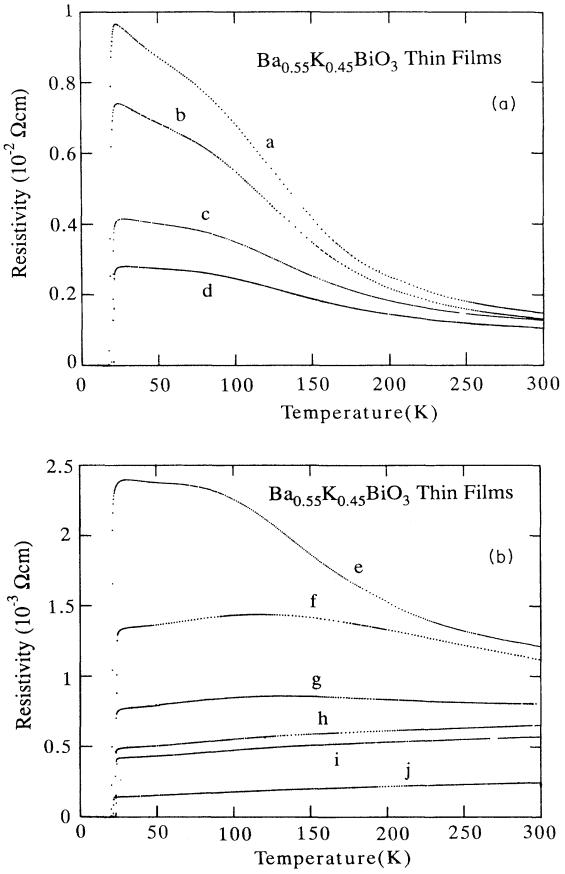

FIG. 1. (a) Temperature dependence of the electrical resistivity for the $Ba_{0.55}K_{0.45}BiO_3$ thin films ($a \sim d$). (b) Temperature dependence of the electrical resistivity for the $Ba_{0.55}K_{0.45}BiO_3$ thin films ($e \sim j$).

TABLE I. The growth conditions of the $Ba_{0.55}K_{0.45}BiO_3$ thin films in Fig. 1 are summarized. (Ag) and (In) in the column for the substrate temperatures mean that the substrates were attached to the heater block by Ag paste and In metal, respectively.

Sample	Substrate	Substrate Temp (°C)	Gas pressure (mTorr)	Annealing conditions Temp (°C)	Cool rate (°C/H)
a	(110)STO	400 (Ag)	8	480	> 100
b	(110)STO	400 (Ag)	12	470	> 100
c	(110)STO	400 (Ag)	8	470	25
d	(110)STO	350 (Ag)	15	470	> 100
e	(110)STO	350 (Ag)	12	460	> 100
f	(110)STO	380 (In)	6	480	> 100
g	(110)STO	500	10	470	> 100
h	(110)STO	320 (Ag)	15	450	25
i	(110)STO	350 (Ag)	12	450	25
j	(110)STO	320 (Ag)	15	460	25

ray-diffraction patterns for these films so that we conclude that the difference in resistivity shown in Fig. 1 arises neither from precipitated impurity phases nor from inhomogeneous distribution of the K content in the films. The current-voltage characteristics in the superconducting state have no feature due to grain-boundary Josephson junctions and the critical current density at 4.2 K was as high as 2×10^5 A/cm^2 even in sample *b* with higher resistivity, indicating that the effect of grain boundaries on the electrical conduction is negligible in these thin films. The difference in the lattice parameter among the films is smaller than the experimental resolution, 0.02%, suggesting the formal valence of Bi ions, namely the number of the charge carriers is almost the same for all of the sample, which is consistent with the result of the Hall measurement described below.

Thus the sample dependence of resistivity should be due to difference in the number of more microscopic lattice imperfections such as dislocations, stacking faults, and antisite defects among the Bi and Ba sites which elastically scatter the charge carriers in $Ba_{0.55}K_{0.45}BiO_3$. The increase in the elastic-scattering rate causes the increase in the temperature-independent part of the resistivity in the metallic films. Moreover the large elastic-scattering rate results in a semiconducting behavior of the resistivity for samples *a*–*g*, signaling a breakdown of the Bloch-Boltzmann-type transport theory for these films as discussed later.

Under appropriate conditions we are able to fabricate thin films reproducibly with almost the same resistivity and T_c as sample *i*, which were mainly used for the measurements of the physical properties described below. We call all of these samples "sample *i*" in the rest of this paper. The resistivity for sample *i* is below 500 $\mu\Omega$ cm even at 300 K.

IV. SUPERCONDUCTING PROPERTIES

We measured the superconducting energy gap in a $Ba_{0.55}K_{0.45}BiO_3$ thin film (sample *i*) by infrared and tunneling spectroscopies. Figure 2 shows the infrared reflectivity spectrum for a thin film in the superconducting state at 5 K divided by that in the normal state at 30 K. The measurements were performed for the thin film placed in a cryostat by a rapid-scan Fourier-type spectrometer. The spectrum consists of a clear peak at 60 cm^{-1} and a broad dip at 135 cm^{-1}.

The normal-state reflectivity spectrum fits well with the Drude curve as will be discussed in Sec. V. When the sample is cooled below $T_c=22.5$ K, the reflectivity increases below 90 cm^{-1}, while it decreases slightly above 90 cm^{-1}. As a result the ratio spectrum, $R_s(\omega)/R_n(\omega)$, exhibits a peak at frequency below 90 cm^{-1} and a broad dip at higher frequency. The positions of the peak observed at 60 cm^{-1} at 5 K shifts to lower frequency as temperature is raised near T_c. The temperature dependence follows that of the superconducting gap energy of the BCS model.

This overall spectral feature and the positions of the peak and the dip show excellent agreement with the previous result reported by Schlesinger *et al.*[10] for a high-density sintered sample with $T_c=26$ K with a transition width of about 4 K. The values of the normalized reflectivity at the peak and the dip are 1.09 and 0.97, respectively, in our data while those in the spectrum measured by Schlesinger *et al.* are 1.05 and 0.98. This slight

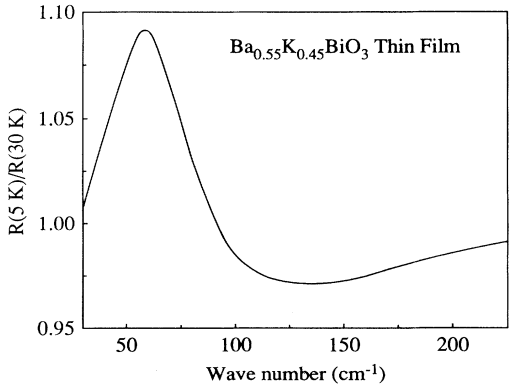

FIG. 2. Reflectivity at 5 K divided by that at 30 K for a $Ba_{0.55}K_{0.45}BiO_3$ thin film (sample *i*).

difference should be due to the fact that the height of the peak and the depth of the dip strongly depend on the normal-state properties such as the damping factor, the carrier number or the effective mass though the position of the peak does not depend on them. Following the analysis by Schlesinger *et al.*,[10] we obtained the superconducting gap $\Delta=3.7\pm0.3$ meV from the normalized reflectivity spectrum. The error is due to the energy resolution of the optical spectrometer.

As pointed out by Schlesinger *et al.*,[10] the spectrum shows a remarkable deviation around the minimum from the calculation using the standard Mattis-Bardeen conductivity,[25] which is valid only in the zero or infinite mean-free-path and extreme weak-coupling limit. Bickers *et al.* showed that a more general Eliashberg calculation[26] with $\lambda\sim1$ provides a better fit to the observed spectra, which is consistent with our estimation of λ as discussed below.

Figure 3(a) shows the current-voltage characteristics for a superconductor-insulator-normal metal (SIN)-type tunnel junction with Au counter electrode fabricated on sample *i* by standard photolithography and ion milling.

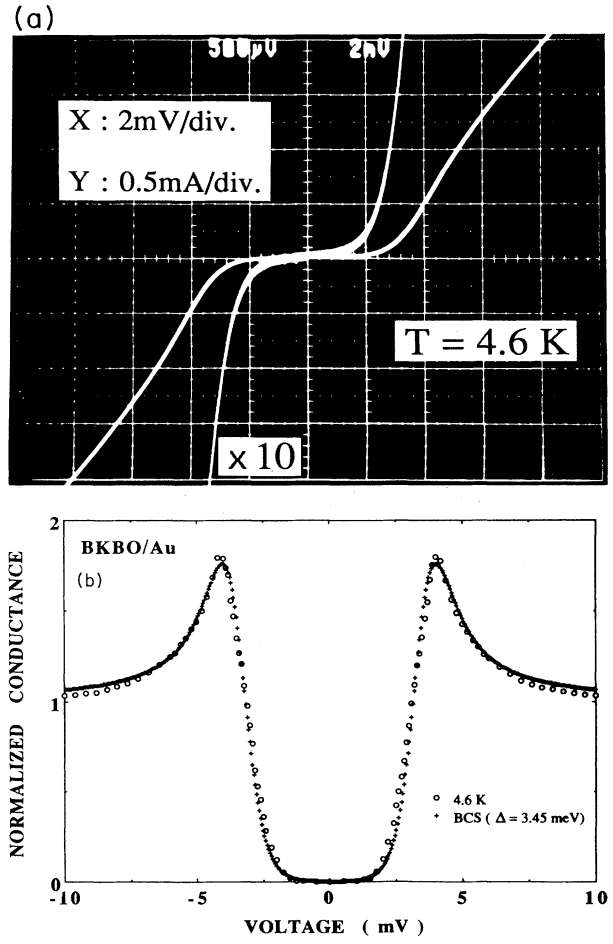

FIG. 3. (a) *I-V* curve for a $Ba_{0.55}K_{0.45}BiO_3$/Au tunnel junction fabricated by standard photolithography and ion milling. (b) Normalized conductance curve derived from the *I-V* curve in (a) by numerical differential.

We formed a natural insulating barrier by exposing the film to the air for 30 min before the evaporation of the Au counter electrode. The zero-bias conductance of the junction in the superconducting state as small as 2% of that in the normal state indicates the higher quality of this junction. The spectrum of the tunneling conductance in Fig. 3(b) obtained by numerical differential from the *I-V* curve can be fitted by the calculated curve using the simple BCS density of states with the superconducting gap $\Delta=3.45$ meV, which coincides with the result of the infrared measurement.

Since far-infrared light penetrates deeply into the film, the superconducting gap determined by infrared measurement is thought to be the value well inside of the film. Therefore, the degradation, if any, in the vicinity of the interface does not affect the infrared gap measurement. We can set the transition temperature of the thin film $T_c=22.5$ K determined by the resistivity measurement for calculation of the ratio of the energy gap to transition temperature and obtain $2\Delta/k_BT_c=3.8\pm0.3$, which is smaller than those in A15 superconductors.[27] Similar values have been reported in the optical measurement[10] and the point-contact tunneling measurement[13] for $Ba_{0.6}K_{0.4}BiO_3$ sintered samples and the tunnel junctions fabricated on thin films grown by molecular-beam epitaxy[16] and a laser deposition method.[18]

We measured the conductance spectra for several tunnel junctions in the bias voltage region from 10 to 100 mV searching for the structure generated by the electron-phonon coupling. Although we observed structure in the energy region from 10 to 25 mV, the amplitude of the structure is smaller than 0.3% of the junction conductance. Moreover the conductance spectrum in the energy region higher than 25 mV is quite monotonous and we could not identify any phonon structure. Sharifi *et al.*[21] also observed no clear phonon structure in the voltage region higher than 20 mV for their sandwich-type tunnel junctions. These results seem to be inconsistent with the estimation of the electron-phonon coupling strength $\lambda\sim1$ discussed below. On the other hand, the tunneling spectrum for point-contact junctions reported by Huang *et al.*[13] exhibited a significant structure in the energy region from 15 to 80 meV.

The disagreement between the results for the thin film junctions and for the point-contact junctions may come from the difference of the junction current density during the measurements. In our thin-film junctions the conductance for the unit area is about one hundred times larger than that in the point-contact junctions.[13] Thus much larger current flowed across the film junctions in the high-bias region and probably smeared out the phonon structure by the heating effect in the vicinity of the junctions.

For the determination of the upper critical field H_{c2} we can use the resistivity measurement, since, as shown in Fig. 4(a), no remarkable broadening of the resistive superconducting transition in the magnetic field was observed in the $Ba_{0.55}K_{0.45}BiO_3$ thin film. This feature is quite different from the case for the sintered sample previously reported[28,29] in which a remarkable tail in the resistive transition was observed at 1 T and the broadening of the

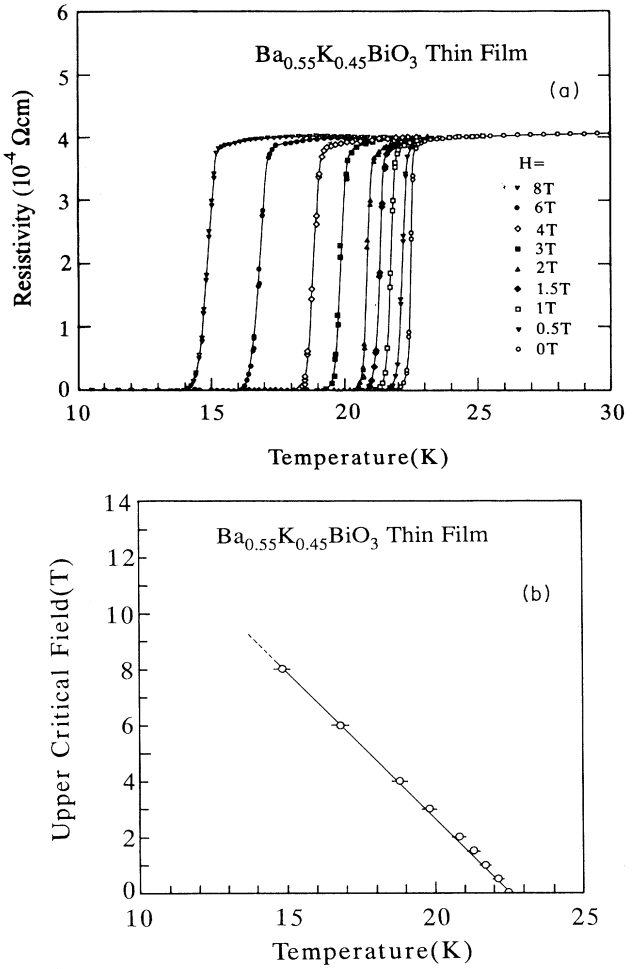

FIG. 4. (a) Resistive superconducting transition in fixed magnetic fields up to 8 T for a $Ba_{0.55}K_{0.45}BiO_3$ thin film (sample *i*). (b) Temperature dependence of H_{c2} determined from (a).

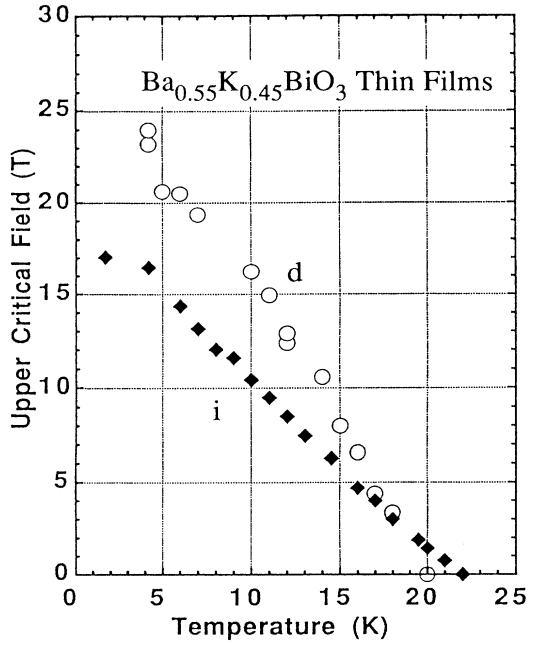

FIG. 5. Temperature dependence of H_{c2} for $Ba_{0.55}K_{0.45}BiO_3$ thin films (sample *i* and sample *d*) determined by a field-sweep measurement with a pulse magnetic-field generating system.

transition grew with increasing field. We can well define the upper critical magnetic field H_{c2} at each temperature from the midpoint of the transition for sample *i* in Fig. 4(a) and plotted in Fig. 4(b). We have extended the measurement of H_{c2} from the magnetic-field dependence of the resistivity at each fixed temperature using a pulsed magnetic field up to 40 T for sample *i* and sample *d*, the latter of which has the room-temperature resistivity 1.1 mΩ cm and negative temperature coefficient of the resistivity. The transition temperature of sample *d* is 20 K. For both samples H_{c2} shows almost linear temperature dependence down to 4.2 K in Fig. 5 though a saturation behavior seems to appear at 1.7 K for sample *i*. The linear dependence of H_{c2} observed here apparently deviates from the concave downward curve calculated from the Werthamer-Helfand-Hohenberg (WHH) theory[30] for the dirty limit, although the overall feature of this material is that of a dirty superconductor. Moreover, there seems to be little effect from the Pauli paramagnetism on H_{c2} in this material, which is known to suppress H_{c2} in a dirty material in the low-temperature region ($T \ll T_c$) below the values expected from the simple WHH curve, which does not take into account the effect of the applied magnetic field on the electron-spin magnetic moments.[31] The previous reports for sintered samples also did not show the concave downward behavior expected from the WHH theory up to 8 T.[28]

The temperature coefficient of H_{c2} at the transition temperature $(dH_{c2}/dT)_{T=T_c}$ is -1.0 T/K for sample *i* and -1.6 T/K for sample *d*. The absolute values of $(dH_{c2}/dT)_{T=T_c}$ observed here are significantly larger than -0.5 T/K previously reported from the magnetic measurement for a powder sample by Batlogg *et al.*,[5] but rather close to -0.79 T/K obtained from the resistive measurement for a high-density sintered sample by Kwok *et al.*[29] This is probably due to the ambiguity in determining the magnetic field at which the magnetization starts to deviate from the value in the normal state as pointed out by Kwok *et al.*[27] H_{c2} at 4.2 K is 17 T for sample *i* and 24 T for sample *d*.

It should be noted that H_{c2} in sample *d* in the low-temperature region is higher than that of sample *i* although the transition temperature of sample *d* is slightly lower. This result seems to be a natural consequence of a superconductivity in the dirty limit in which the upper critical field is enhanced by a short mean free path. As discussed above, a linear extrapolation of H_{c2} to 0 K consistent with the Ginzburg-Landau (GL) theory may be more appropriate than to WHH formula. The corresponding critical field is $H_{c2}(0)=23$ T and the GL coherence length is $\xi_{GL}(0)=37$ Å for sample *i* in Fig. 4(b).

V. NORMAL-STATE PROPERTIES

In our previous work on the x dependence of the optical spectrum,[15] we have suggested that the destruction of the CDW gap in the metallic $Ba_{1-x}K_xBiO_3$ restores the original O $2p$ and Bi $6s$ hybridized conduction band with less than half-filling, just what one expects from the band theory[23] but completely different from the picture where the holes are doped into the parent insulator $BaBiO_3$ by K substitution. The measurement of the normal-state properties performed in this work confirmed the previous result.

As shown in Fig. 6, the Hall coefficients for two of the $Ba_{0.55}K_{0.45}BiO_3$ thin films, samples g and i, are negative in sign suggesting the charge carriers are electrons. The values of the Hall coefficient $R_H = -3 \sim 4 \times 10^{-4}$ cm^3/C are about twice smaller than the expected value from a simple free-electron gas model based on the band picture. Nevertheless the smaller value can be explained by band theory considering the anisotropy in the scattering of the charge carriers.[32] Note that the values of R_H are nearly identical in both samples, whereas the resistivity is by a factor of more than 2 different. Therefore, the difference in resistivity is mainly due to the difference in the mobility. For a more precise discussion on the consistency between the Hall coefficient and the band theory, an investigation for the composition (x) dependence of R_H in the $Ba_{1-x}K_xBiO_3$ system is necessary but such a study has not been done yet. The temperature dependence of R_H is small as seen in typical metals and shows a good agreement between samples g and i.

The optical reflectivity spectrum at room temperature for sample i is shown in Fig. 7. The spectrum does not show a large deviation from the Drude curve shown by the solid line from far-infrared to visible region. The best-fit Drude parameters are the bare plasma energy $(\sqrt{\varepsilon_\infty})\omega_p = 2.9$ eV and the damping factor $\gamma = 1.0$ eV. The conductivity at $\omega = 0$, $\sigma(0) = \varepsilon_\infty \omega_p^2/\gamma = 2 \times 10^3$ Ω^{-1}cm^{-1}, derived from the fitting parameters is in fair agreement with the dc conductivity of this film.

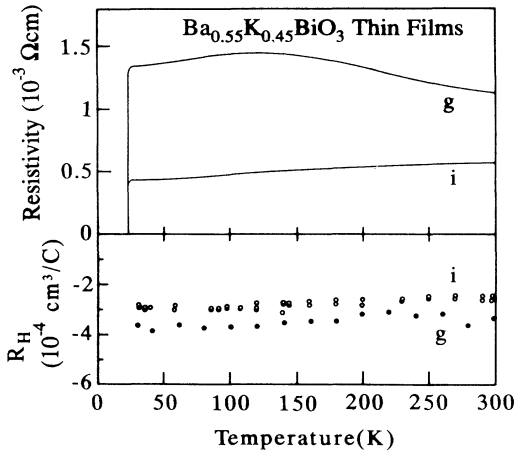

FIG. 6. Hall coefficient and electrical resistivity for $Ba_{0.55}K_{0.45}BiO_3$ thin films (sample i and sample g).

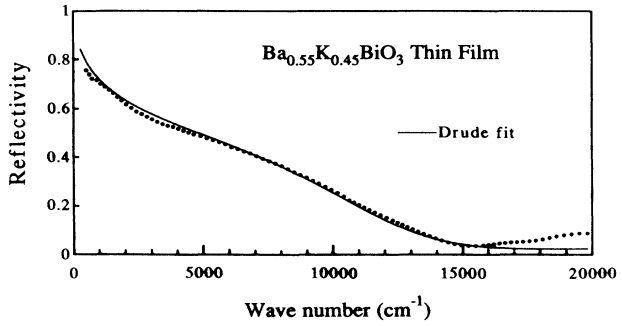

FIG. 7. Reflectivity spectrum at room temperature for a $Ba_{0.55}K_{0.45}BiO_3$ thin film (sample i). The solid line is a curve calculated by a Drude model with the parameters given in the text.

It should be noted that the damping factor of 1.0 eV is quite large, which gives rise to serious doubt whether the optical conductivity can be described by Drude theory for a single free-carrier band. We do not have experimental results to answer this question in the present stage.

Nevertheless, the fact that the deviation of the reflectivity from the Drude curve is significantly smaller than in the predecessor $BaBi_{0.25}Pb_{0.75}O_3$ (Ref. 34) and/or the superconducting cuprates (Ref. 35) strongly suggests that the splitting of the conduction band observed in $BaBiO_3$ disappears and a conduction band with density of states expected from the band calculation is realized in $Ba_{0.55}K_{0.45}BiO_3$. In $BaBi_{0.25}Pb_{0.75}O_3$, the optical spectrum shows a pronounced deviation from the Drude curve, which is a consequence of the persistence of the CDW gap even in the metallic phase. Our data do not rule out a small deviation in the lowest energy region as pointed out by Schlesinger and co-workers,[10,33] but we suppose that this may not be intrinsic and further improvement in the sample homogeneity would diminish the deviation from the Drude curve.

In order to further characterize the electronic and/or phonon states we have measured the Raman-scattering spectra for both metallic and insulating samples. The spectra shown in Fig. 8 were measured at room temperature in the backscattering configuration using 5145-Å beam from an Ar laser. Details were described in the preceding paper by Tajima *et al.*[36] The Raman spectrum of the parent insulator $BaBiO_3$ is dominated by an extremely strong peak at 570 cm^{-1} with higher harmonics. This peak was assigned to the breathing mode of the oxygen octahedra surrounding Bi atoms.[37] In an ideal (undistorted) cubic perovskite structure there is no Raman-active optical phonon—forbidden by the selection rule. The anomalously strong intensity of the breathing-mode phonon in $BaBiO_3$ arises from the static breathing-mode distortion coupled with the resonant electronic excitation across the CDW gap ($\sim$2 eV).[38]

As the K composition increases, the intensity of the 570-cm^{-1} peak is reduced and finally disappears in the metallic phase. The decrease in intensity is partly due to the decrease in the CDW gap energy which makes the scattering off resonant. At the metallic compositions, the

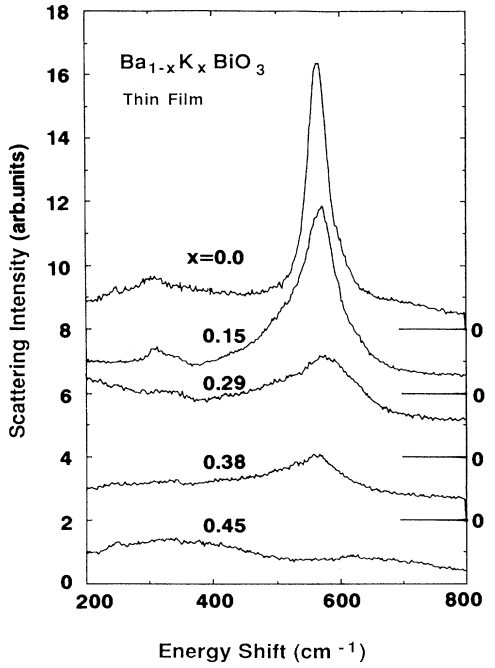

FIG. 8. Raman spectra at room temperature for $Ba_{1-x}K_xBiO_3$ thin films with a 5145-Å Ar-laser excitation.

570-cm^{-1} peak disappears almost completely, though some peak features are seen at different frequencies, the origin of which is not clear at present. The structural analysis indicates a cubic symmetry for the metallic $Ba_{1-x}K_xBiO_3$. However, as far as the breathing-mode distortion remains, the breathing-mode phonon is Raman active even in the cubic symmetry (O_h^5).[36] Therefore, the disappearance of the 570-cm^{-1} peak is an indication that $Ba_{1-x}K_xBiO_3$ recovers an ideal cubic perovskite structure without breathing-mode lattice distortion in the metallic phase, consistent with the result of the x-ray structural characterization on single crystals[38] as well as the neutron structural study.[24] This conclusion from the Raman study is compatible with the various experimental facts shown above.

The negative Hall coefficient and disappearance of the 570-cm^{-1} peak in the Raman spectrum indicate destruction of the CDW gap in the metallic $Ba_{1-x}K_xBiO_3$, which strongly suggests restoration of the conduction band expected from the band calculation for this material. Moreover the reflectivity spectrum is also consistent with this band picture if we assume that the motion of the charge carriers in this material can be described by a Drude form.

VI. DISCUSSION

Considering the experimental results shown above it is a good approximation to assume that the electronic structure in $Ba_{0.55}K_{0.45}BiO_3$ can be described by band theory. By this assumption and the BCS formulas, the mean free path is estimated from the superconducting-state properties and the normal-state properties, respectively.

Using the Fermi velocity v_F extracted from the result of band calculation,[23] we obtained the Pippard length $\xi_0=hv_F/2\pi^2\Delta=570$ Å from the superconducting energy gap $\Delta=3.7$ meV for sample *i*. The GL coherence length $\xi_{GL}(0)=37$ Å in this sample is calculated from the linear temperature dependence of H_{c2}. Thus $Ba_{0.55}K_{0.45}BiO_3$ is a dirty-limit superconductor with the mean free path $l \ll \xi_0$. The mean free path $l=6.9$ Å is estimated by the formula for the dirty limit in the BCS theory from ξ_0 and $(dH_{c2}/dT)_{T=T_c}$.

On the other hand $l=mv_F/ne^2\rho=7$ Å and is directly estimated from the measured resistivity ρ at 30 K using the carrier number n, the effective mass m and v_F from the band calculation.[23] Moreover, if we assume that the optical conductivity is described by a Drude form, $l=hv_F/2\pi\gamma=7$ Å is also derived from the scattering rate γ in the plasma spectrum at 300 K.

These three estimations from independent measurements coincide well with each other. This internal consistency between the normal-state parameters and the superconducting parameters justifies the validity of both the above assumption and the description of the superconductivity in this system based on the BCS theory.

The estimation of the mean free path from the resistivity measurement also provides an explanation for the clear correlation between the magnitude and the temperature dependence of resistivity for the $Ba_{0.55}K_{0.45}BiO_3$ thin films in Fig. 1. In the samples with the room-temperature resistivity lower than 700 $\mu\Omega$ cm, the temperature dependence of resistivity is metallic with positive temperature coefficient. When the room-temperature resistivity of the sample exceeded 700 $\mu\Omega$ cm, the temperature dependence of resistivity exhibits a semiconductor-like behavior. The critical resistivity 700 $\mu\Omega$ cm corresponds to the mean free path equal to the lattice parameter 4 Å. This is consistent with the general trends that the lower bound of mean free path in Bloch-Boltzmann transport theory is set by lattice parameter,[38] thus giving an evidence that the present films are homogeneous and the transport properties are not affected by macroscopic inhomogeneity such as grain boundary or inhomogeneous distribution of the K composition. Actually the mean free path for sample *d* used for the H_{c2} measurement is estimated to be $l=4$ Å or less by the same procedure as used for sample *i*.

The physical parameters for $Ba_{0.55}K_{0.45}BiO_3$ derived here were summarized in Table II together with the values for $BaBi_{0.25}Pb_{0.75}O_3$ ($T_c=12$ K) for comparison.[40,41] The mean free path for $BaBi_{0.25}Pb_{0.75}O_3$ is supposed to be close to the lattice constant 4.2 Å from the fact that the resistivity for this material shows a semiconductorlike behavior with a negative temperature coefficient. The Pippard length ξ_0 was calculated from the superconducting energy gap Δ and the Fermi velocity based on the simple band picture for both materials. It can be seen that the $(dH_{c2}/dT)_{T=T_c}$ for $BaBi_{0.25}Pb_{0.75}O_3$ is about half of that for $Ba_{0.55}K_{0.45}BiO_3$. The value of $(dH_{c2}/dT)_{T=T_c}$ is even smaller than that expected from

TABLE II. Physical parameters for $Ba_{0.55}K_{0.45}BiO_3$ (sample *i*) and $BaBi_{0.25}Pb_{0.75}O_3$.

	$Ba_{0.55}K_{0.45}BiO_3$	$BaBi_{0.25}Ph_{0.75}O_3$
T_c (K)	22.5	12[a]
Δ (meV)	3.7±0.3	1.65[a]
$(dH_{c2}/dT)_{T=T_c}$ (T/K)	−1.0	−0.53[b]
ξ_0 (Å)	570	900[c]
$\xi_{GL}(0)$ (Å)	37	70[b]
l (Å)	6.9	~4[c]

[a]Reference 39.
[b]Reference 40.
[c]See the text.

the Pippard length and the mean free path. In $BaBi_{0.25}Pb_{0.75}O_3$, the experimental results[34] have suggested that the persistence of the CDW distorts the conduction band and generates a pseudogap around the Fermi level. The discrepancy between the experimental result and the calculation based on the simple band picture may be explained by this distortion of the conduction band. By contrast, the consistency of parameters of $Ba_{0.55}K_{0.45}BiO_3$ with the band theory and the BCS theory indicates the almost perfect restoration of the simple band picture upon K substitution for $BaBiO_3$.

Both Bi-based materials are dirty superconductors and the short mean free path makes $\xi_{GL}(0)$ in these materials as short as the in-plane coherence length in the Cu-based superconducting oxides. The Cu-oxide superconductors are rather clean [$\xi_{GL}(0) < l$] and the short coherence length is due to the short Pippard length.

Finally we would like to attempt to estimate the strength of the electron-phonon coupling in $Ba_{0.55}K_{0.45}BiO_3$. First, we can estimate conventionally the coupling constant λ from the gap measurement. Following the numerical studies based on the Eliashberg equations,[27,42] $2\Delta/k_BT_c = 3.8\pm0.3$ obtained in this work corresponds to $0 < \lambda < 1$. Although the accuracy of the data is not enough to determine the exact value of λ, the upper bound of λ may be set around 1. Another source for the estimation of the strength of the electron-phonon coupling is the temperature dependence of the electrical resistivity.[43] In the temperature region much higher than the Debye temperature, the Bloch-Boltzmann resistivity approaches to a straight line with the slope $d\rho/dT = \lambda/(0.246\varepsilon_\infty \langle \omega_p^2 \rangle)$.[44] The slope of 0.26 $\mu\Omega$ cm/K at 300 K for the $Ba_{0.55}K_{0.45}BiO_3$ thin films observed in this work corresponds to $\lambda \sim 0.6$ with $\varepsilon_\infty \omega_p^2 = (2.9\ \text{eV})^2$ estimated from the optical measurement. There is a large ambiguity also in this estimation due to the lack of the resistivity data in the high-temperature region and sufficient understanding of the transport mechanism in this material. Especially it is suggested that the case with a very short mean free path requires a large correction to value of λ.[43] The corrected value of λ is about two times larger than the uncorrected value in the case of A15's.[43] Actually the slope at 300 K does not extrapolate to the resistivity at T_c but to a value 20% higher than that. Nevertheless the estimation of λ from the resistivity seems to be consistent with the gap measurement and suggest that λ is around 1.

Recently Huang *et al.*[13] performed a gap-inversion analysis on their point-contact tunneling data and extracted $\lambda \sim 1$ and $2\Delta/k_BT_c = 3.8 \sim 3.9$. The numerical study on the superconductivity in $Ba_{1-x}K_xBiO_3$ by Jin *et al.*[45] is fairly successful in explaining the whole experimental data including the result by Huang *et al.* based on a model of the electron-phonon Eliashberg function. Shirai, Suzuki, and Moitzuki[46] also extracted $\lambda = 0.8$ for $Ba_{0.6}K_{0.4}BiO_3$ from a numerical calculation based on the tight-binding model with parameters estimated from the band calculation.[23] Our estimation is also consistent with them.

VII. SUMMARY

In summary, we have performed an extensive study on the superconducting- and normal-state properties of $Ba_{1-x}K_xBiO_3$ thin films. Through the quantitative analyses on the experimental results, we conclude that the density of states of the conduction band in $Ba_{1-x}K_xBiO_3$ is close to that calculated by the band theory in its metallic phase, and the superconductivity is of BCS-type in the dirty limit as previously suggested from the studies for bulk samples. The gap measurements and the slope of the resistivity suggest $\lambda \sim 1$.

This result is quite in contrast to the case of the copper-oxide superconductors, in which the electronic states are largely distorted from the simple band picture by the strong electron correlation and there has not been established any theory which connects the parameters for the normal state with those for the superconducting state. It would be meaningful that the study for $Ba_{1-x}K_xBiO_3$ has confirmed that the conventional weak- or moderate-coupling BCS mechanism can be responsible for high-T_c value of the order of 30~40 K.

ACKNOWLEDGMENTS

One of the authors (H.S.) would like to thank M. Naito and E. S. Hellman for helpful discussions.

*Present address: NTT Basic Research Laboratories, Midoricho 3-9-11, Musashino-shi, Tokyo 180.

[1]L. F. Mattheiss, E. M. Gyorgy, and D. W. Johnson, Jr., Phys. Rev. B **37**, 3745 (1988).
[2]R. J. Cava, B. Batlogg, J. J. Krajewski, R. Farrow, L. W. Rupp, Jr., A. E. White, K. Short, W. F. Peck, and T. Komeotani, Nature (London) **332**, 814 (1988).
[3]A. F. Hebard, M. J. Rosseinski, R. C. Haddon, D. W. Murphy, S. H. Glarum, T. T. M. Palstra, A. P. Ramirez, and A. R. Kortan, Nature (London) **350**, 600 (1991).
[4]D. G. Hinks, B. Dabrowski, J. D. Jorgensen, A. W. Mitchell, D. R. Richards, S. Pei, and D. Shi, Nature (London) **333**, 836

(1988).
[5]B. Batlogg, R. J. Cava, L. W. Rupp, Jr., A. M. Mujsce, J. J. Krajewski, J. P. Remeika, W. F. Peck, Jr., A. S. Cooper, and G. P. Espinosa, Phys. Rev. Lett. **61**, 1670 (1988).
[6]Y. J. Uemura, B. J. Sternlieb, D. E. Cox, J. H. Brewer, R. Kadono, J. R. Kempton, R. F. Kiefl, S. R. Kreitzman, G. M. Luke, P. Mulhern, T. Riseman, D. L. Williams, W. J. Kossler, X. H. Yu, C. E. Stronach, M. A. Subramanian, J. Gopalakrihnaan, and A. W. Sleight, Nature (London) **335**, 151 (1988).
[7]D. G. Hinks, D. R. Richards, B. Dabrowski, D. T. Marx, A. W. Mitchell, Nature (London) **335**, 419 (1988).
[8]S. Kondoh, M. Sera, Y. Ando, and M. Sato, Physica C **157**, 469 (1989).
[9]D. G. Hinks, A. W. Mitchell, Y. Zheng, D. R. Richards, and B. Dabrowski, Appl. Phys. Lett. **54**, 1585 (1989).
[10]Z. Schlesinger, R. T. Collins, J. A. Caleise, D. G. Hinks, A. W. Mitchell, Y. Zheng, B. Dabrowski, N. E. Bickers, and D. J. Scalapino, Phys. Rev. B **40**, 6862 (1989).
[11]K. F. McCarty, H. B. Radouski, D. G. Hinks, Y. Zheng, A. W. Mitchell, T. J. Folkerts, and R. N. Shelton, Phys. Rev. B **40**, 2662 (1989).
[12]J. F. Zasadzinski, N. Tralshawala, D. G. Hinks, B. Dabrowski, A. W. Mitchell, and D. R. Richards, Physica C **158**, 519 (1989).
[13]Q. Huang, J. F. Zasadzinski, N. Tralshawala, K. E. Gray, D. G. Hinks, J. L. Peng, and R. L. Greene, Nature (London) **347**, 369 (1990).
[14]S. Kondoh, M. Sera, K. Fukuda, Y. Ando, and M. Sato, Solid State Commun. **67**, 879 (1988).
[15]H. Sato, S. Tajima, H. Takagi, and S. Uchida, Nature (London) **338**, 241 (1989).
[16]E. S. Hellman, E. H. Hartford, Jr., and R. M. Fleming, Appl. Phys. Lett. **55**, 2120 (1989).
[17]M. Iyori, M. Kamino, K. Takahashi, Y. Yoshisato, and S. Nakano, Physica C **185-189**, 1965 (1991).
[18]B. M. Moon, C. E. Platt, R. A. Schweinfurth, and D. J. Van Harlingen, Appl. Phys. Lett. **59**, 1905 (1991).
[19]M. L. Norton, Mater. Res. Bull. **24**, 1391 (1989).
[20]H. Sato, H. Takagi, and S. Uchida, Physica C **169**, 391 (1990).
[21]F. Sharifi, A. Pargellis, R. C. Dynes, B. Miller, E. S. Hellman, J. Rosamilia, and E. H. Hartford, Jr., Phys. Rev. B **44**, 12 522 (1991).
[22]H. Sato, S. Tajima, H. Takagi, and S. Uchida, Phys. Rev. Lett. **162**, 1121 (1989).
[23]L. F. Mattheiss and D. R. Hamann, Phys. Rev. Lett. **60**, 2681 (1988).
[24]S. Pei, J. D. Jorgensen, D. G. Hinks, D. R. Richards, A. W. Mitchell, J. M. Newsam, S. K. Sinha, D. Vaknin, and A. J. Jacobson, Phys. Rev. B **41**, 4126 (1990).
[25]D. C. Mattis and J. Bardeen, Phys. Rev. **111**, 412 (1958).
[26]E. Bickers, D. J. Scalapino, R. T. Collins, and Z. Schlesinger (unpublished).
[27]F. Marsiglio and J. P. Carbotte, Phys. Rev. B **33**, 6141 (1986).
[28]U. Welp, W. K. Kwok, G. W. Crabtree, H. Claus, K. G. Vandervoort, B. Dabrowski, A. W. Mitchell, D. R. Richards, D. T. Marx, and D. G. Hinks, Physica C **156**, 27 (1988).
[29]W. K. Kwok, U. Welp, G. W. Crabtree, K. G. Vandervoort, R. Hulscher, Y. Zheng, B. Dabrowski, and D. G. Hinks, Phys. Rev. B **40**, 9400 (1989).
[30]N. R. Werthamer, E. Helfand, and P. C. Hohenberg, Phys. Rev. **147**, 288 (1966).
[31]N. R. Werthamer, E. Helfand, and P. C. Hohenberg, Phys. Rev. **147**, 295 (1966).
[32]N. Hamada, S. Massidda, J. Yu, and A. J. Freeman, Phys. Rev. B **42**, 6238 (1990).
[33]S. H. Blanton, R. T. Collins, K. H. Kelleher, L. D. Rotter, Z. Schlesinger, D. G. Hinks, and Y. Zheng, Phys. Rev. B **47**, 996 (1993).
[34]S. Tajima, S. Uchida, A. Masaki, H. Takagi, K. Kitazawa, S. Tanaka, and A. Katsui, Phys. Rev. B **32**, 6302 (1985).
[35]For example, J. Orenstein, G. A. Thomas, A. J. Millis, S. L. Cooper, D. H. Rapkine, T. Timusk, L. F. Schneemeyere, and J. V. Waszczak, Phys. Rev. B **42**, 6342 (1990); Z. Schlesinger, R. T. Collins, F. Holtzberg, C. Feild, G. Koren, and A. Gupta, Phys. Rev. B **41**, 11 237 (1990).
[36]S. Tajima, M. Yoshida, N. Koshizuka, H. Sato, and S. Uchida (unpublished).
[37]S. Sugai, S. Uchida, K. Kitazawa, S. Tanaka, and A. Katsui, Phys. Rev. Lett. **55**, 426 (1985); S. Uchida, K. Kitazawa, and S. Tanaka, Phase Trans. **8**, 95 (1987).
[38]L. F. Schneemeyer, J. K. Thomas, T. Siegrift, B. Batlogg, L. W. Rupp, R. L. Opsla, R. J. Cava, and D. W. Murphy, Nature (London) **335**, 421 (1988).
[39]N. F. Mott, *Metal-Insulator Transition* (Taylor and Francis, London, 1974).
[40]B. Batlogg, Physica B **126**, 275 (1984).
[41]K. Kitazawa, S. Uchida, and S. Tanaka, Physica B **135**, 505 (1985).
[42]P. B. Allen and R. C. Dynes, Phys. Rev. B **12**, 905 (1975).
[43]M. Gurvitch, Physica **135B**, 276 (1985).
[44]P. B. Allen, Phys. Rev. B **3**, 305 (1971).
[45]W. Jin, M. H. Degani, R. K. Kalia, and P. Vashishta, Phys. Rev. B **45**, 5535 (1992).
[46]M. Shirai, N. Suzuki, and K. Motizuki, J. Phys.:Condens. Matter **2**, 3553 (1990).